~~CONFIDENTIAL~~

LWP - 939
Copy No. 34

LWP - 939

LANGLEY WORKING PAPER

PRELIMINARY WIND-TUNNEL INVESTIGATION OF THE EFFECTS OF ENGINE NACELLES ON A TRANSPORT CONFIGURATION WITH HIGH LIFT-DRAG RATIOS TO A MACH NUMBER OF 1.00

By Stuart G. Flechner

Langley Research Center
Hampton, Virginia

(NASA-TM-82312) PRELIMINARY WIND-TUNNEL INVESTIGATION OF THE EFFECTS OF ENGINE NACELLES ON A TRANSPORT CONFIGURATION WITH HIGH LIFT DRAG RATIOS TO A MACH NUMBER OF 1.00 (NASA) 20 p HC A02/MF A01 CSCL 01C G3/05 N81-19099 Unclas 19105

and is subject to possible incorporation in a formal NASA report.

LWP - 939

February 16, 1971

LANGLEY WORKING PAPER

PRELIMINARY WIND-TUNNEL INVESTIGATION OF THE EFFECTS OF ENGINE NACELLES ON A TRANSPORT CONFIGURATION WITH HIGH LIFT-DRAG RATIOS TO A MACH NUMBER OF 1.00

Prepared by

Stuart G. Flechner

Approved by

Mark R. Nichols
Chief, High-Speed Aircraft Division

Approved for distribution by

Laurence K. Loftin, Jr.
Director for Aeronautics

LANGLEY RESEARCH CENTER

NATIONAL AERONAUTICS AND SPACE ADMINISTRATION

[redacted]

[redacted]

NATIONAL AERONAUTICS AND SPACE ADMINISTRATION

Working Paper No. 939

PRELIMINARY WIND-TUNNEL INVESTIGATION OF THE EFFECTS OF ENGINE NACELLES ON A TRANSPORT CONFIGURATION WITH HIGH LIFT-DRAG RATIOS TO A MACH NUMBER OF 1.00

By Stuart G. Flechner

SUMMARY

An investigation was conducted in the Langley 8-foot transonic pressure tunnel to determine the effect of engine nacelles added to a low-wing—fuselage—vertical-tail configuration utilizing the NASA supercritical airfoil and a refined area ruled fuselage. The engine arrangement consisted of two aft fuselage, side mounted flow-through nacelles and a solid body-of-revolution mounted above the fuselage in a manner similar to the Boeing 727.

A preliminary analysis of the wind-tunnel data shows that favorable interference drag can be obtained with the proper longitudinal locations of the nacelles, by canting the nacelle inlets. and by cusping the rearward region of the nacelle.

INTRODUCTION

Reference 1 presented wind-tunnel results for a low-wing—fuselage—vertical-tail configuration utilizing the NASA supercritical airfoil and a fuselage shaping based on an area rule refined to account for second order effects. High lift-to-drag ratios to $M = 1.00$ were achieved.

~~CONFIDENTIAL~~

The present preliminary investigation was conducted to determine the effects of added engine nacelles on the aerodynamic characteristics of the configuration of reference 1. The engine arrangement was similar to that of the Boeing 727. The two fuselage, side-mounted engines were simulated by flow-through nacelles. The center engine was simulated by a solid body-of-revolution.

The results presented herein indicate the effects of shifting the simulated engines longitudinally, canting the nacelle inlets, and cusping the rearward region of the nacelles. This investigation was conducted at Mach numbers of 0.98 and 1.00 near the design lift coefficient of 0.40. Also presented is the effect of replacing the flow-through nacelles with their equivalent cross-sectional areas added to the sides of the fuselage. This configuration, to obtain the nacelle-fuselage interference effect, was tested at Mach numbers from 0.80 to 1.00 at lift coefficients from approximately 0.25 to 0.51.

SYMBOLS

The results presented are referenced to the model stability axis and the geometry as presented in reference 1. The coefficients and symbols used herein are defined as follows:

C_L lift coefficient, Lift/qS

ΔC_D difference in drag coefficient for two configurations at the same lift coefficient

M free-stream Mach number

q free-stream dynamic pressure, N/m^2

S wing reference area (basic panel) including the fuselage intercept, 0.1928 m^2

APPARATUS AND PROCEDURES

Tunnel

The investigation was conducted in the Langley 8-foot transonic pressure tunnel which is a single return tunnel having a rectangular slotted test section. The tunnel has the capability for the independent variation of Mach number, density, temperature, and humidity. Significant condensation effects were avoided by maintaining sufficient values of stagnation temperature and dewpoint. In addition to the normal 6-percent open slotted top and bottom walls, special side wall inserts were used on the solid side walls. These inserts are indented in the region of the model with 40-percent of the cross-sectional area of the model removed to account for the sideward displacement of the air by the model.

Model

Model drawings are shown in figure 1 and photographs are presented in figure 2. The ripple effect along the bottom of the fuselage aft end and the screw at the base of the fuselage, shown in the model photographs, were due to the model support system used for photographic purposes only. Details of the original model are given in reference 1. The additional cross-sectional area of the nacelles was removed from the fuselage thus maintaining the original cross-sectional area distribution. The flow-through nacelle area distribution, shown in figure 3, has the inside stream tube cross-sectional area removed. The middle nacelle, the body of revolution, has the same area as a flow-through nacelle. The nose is located 8.890 centimeters forward of the side nacelle inlets.

[redacted]

The basic fuselage of reference 1 was shortened by 6.604 centimeters and a new, thick, vertical tail was used to accomodate the middle nacelle. All cross-sectional area changes to the fuselage were accomplished by changing the width and maintaining approximate elliptical cross sections. A fixed horizontal T-tail was used throughout this present investigation.

Nacelle location.- In addition to the basic configuration as shown in figure 1(a), the three nacelles were tested in a position 5.080 centimeters rearward. The fuselage was reshaped to conform to the area distribution as shown in figure 4 of reference 1.

Inlet cant.- The basic nacelle inlet has a cant of approximately 16°. To determine the effect of the cant, a straight inlet was also tested. Coordinates are listed in Table I (see figure 1(b)).

Nacelle cusp.- The basic nacelle has a slight cusp near the aft end. To determine the effects of the cusp, a portion of the investigation was conducted with the cusp filled in and smoothly faired to the rest of the nacelle. Coordinates are listed in Table I (see figure 1(b)).

Equivalent body.- The equivalent body was used to determine the fuselage-engine interference effect. The flow-through nacelles were removed from the pylons and the fuselage was widened to maintain the same area distribution (see figure 1(c)).

Pylon.- The length, thickness, and width (at the nacelle trailing edge) of the pylon were changed slightly during the investigation. For the data presented herein, the pylon was not changed during each change to obtain the drag differential, ΔC_D. For the whole investigation, the sharp pylon leading edge was maintained 5.080 centimeters aft of the

[redacted]

nacelle leading edge. The pylon leading-edge width was also maintained at 0.864 centimeters. The fuselage was contoured to provide a constant channel between the nacelle and the fuselage after the boundary-layer displacement and pylon thickness were taken into account.

Boundary-Layer Transition

Using the technique described in reference 1, the flow-through nacelles had a strip of number 220 carborundum grains applied 0.508 centimeters behind the straight inlet leading edge and 23.526 centimeters forward of the trailing edge of the canted inlet nacelle. The strips were applied inside and outside. The body-of-revolution had a strip of number 150 grains applied 1.905 centimeters behind the nose.

Measurements

Aerodynamic forces and moments were measured with an internally mounted six-component strain-gage balance. The pressure in the vicinity of the base of the model and in the balance cavity were also measured. These pressures were used to adjust the drag results to correspond to free-stream static pressure acting at the model base and in the balance cavity.

For the basic configuration and the equivalent body, data were obtained at Mach numbers of 0.80, 0.90, 0.95, and 1.00, over the lift coefficient range from approximately 0.25 to 0.51. The other configurations had data obtained only at Mach numbers of 0.98 and 1.00 near the design cruise lift coefficient of 0.40.

[redacted]

PRESENTATION OF RESULTS

The incremental drag, ΔC_D, shown in figures 4, 5, and 6 were computed as follows:

Nacelle Location Effect.- The forward location configuration drag subtracted from the rearward location drag.

Nacelle Inlet Cant Effect.- The drag of the nacelle canted inlet configuration subtracted from that of the straight inlet.

Nacelle Cusp Effect.- The cusped nacelle configuration drag subtracted from the filled-in configuration.

Interference Effect.- The drag of the equivalent body subtracted from the drag of the basic configuration. (The basic configuration has cusped nacelles with canted inlets located in the forward position.)

Thus, positive ΔC_D is the drag penalty for having the nacelles in the rear position, for having straight nacelle inlets, for not cusping the nacelle, and for having the nacelles on the body.

DISCUSSION OF RESULTS

Nacelle location.- Figure 4(a) shows the penalty for having the nacelles in the rearward position. The penalty at $M = 1.00$ is substantial; 0.0010 at the design lift coefficient. At and below the design lift coefficient, for $M = 0.98$, the rear nacelle position is slightly more favorable than the forward position.

Inlet cant.- The canted nacelle inlet has less drag than the straight inlet, the differential drag coefficient being 0.0005 at the design point.

[redacted]

Nacelle cusp.- The effects of the cusp were not as pronounced as the effects of the other nacelle changes. At M = 0.98 there is a small benefit for using cusped nacelles. At M = 1.00, below the design lift coefficient, there is a small penalty for using cusped nacelles.

Interference effects.- Figure 5 shows the drag increment that is due to the flow-through nacelles over the larger Mach number and lift coefficient ranges. This increment is shown for the design lift coefficient of 0.40 versus Mach number in figure 6. Also plotted is the skin friction, computed from compressible flow theory. This shows a favorable interference drag of 0.0005 at M = 1.00.

CONCLUDING REMARKS

By properly adding nacelles to an existing optimum configuration, favorable interference drag can be obtained. At the design lift coefficient of 0.40 and at a Mach number of 1.00, favorable interference drag was obtained by considering the following factors:

1. Nacelle location - an excessively rearward location on the fuselage is unfavorable.

2. Nacelle inlet - canting the inlet was more favorable than a straight inlet.

3. Nacelle contour - cusping along the rearward region was generally more favorable.

[redacted]

REFERENCES

1. Langhans, Richard A.; and Whitcomb, Richard T.: Preliminary Wind-Tunnel Investigation of a Low-Wing—Fuselage—Vertical-Tail Configuration With High Lift-Drag Ratios at Mach Numbers to 1.00. Langley Working Paper No. 898, September 15, 1970.

[redacted]

[redacted]

TABLE I.- FLOW-THROUGH NACELLE COORDINATES

Station cm.	Outside Radius, cm.			
	Inlet			
	Straight	Canted		
		Inboard Side	Outboard Side	Top And Bottom
-1.45			2.54	
-0.75			2.64	2.54
0.0	2.54	2.54	2.80	2.69
1.0	2.80	2.80	2.90	2.85
2.0	2.96	2.96	3.00	2.98
3.0	3.04	3.04	3.11	3.08
4.0	3.16	3.16	3.19	3.18
5.0	3.18	3.18	3.20	3.19
6.0	3.20	3.20	3.22	3.21

	Rear Portion	
	Uncusped	Cusped
7.0	3.22	3.22
8.0	3.21	3.21
9.0	3.20	3.20
10.0	3.15	3.15
11.0	3.10	3.10
12.0	3.06	3.00
13.0	2.97	2.90
14.0	2.88	2.80
15.0	2.77	2.71
16.0	2.68	2.65
17.0	2.56	2.55
17.55	2.48	2.48

ID = 4.93 cm.

[redacted]

[redacted]

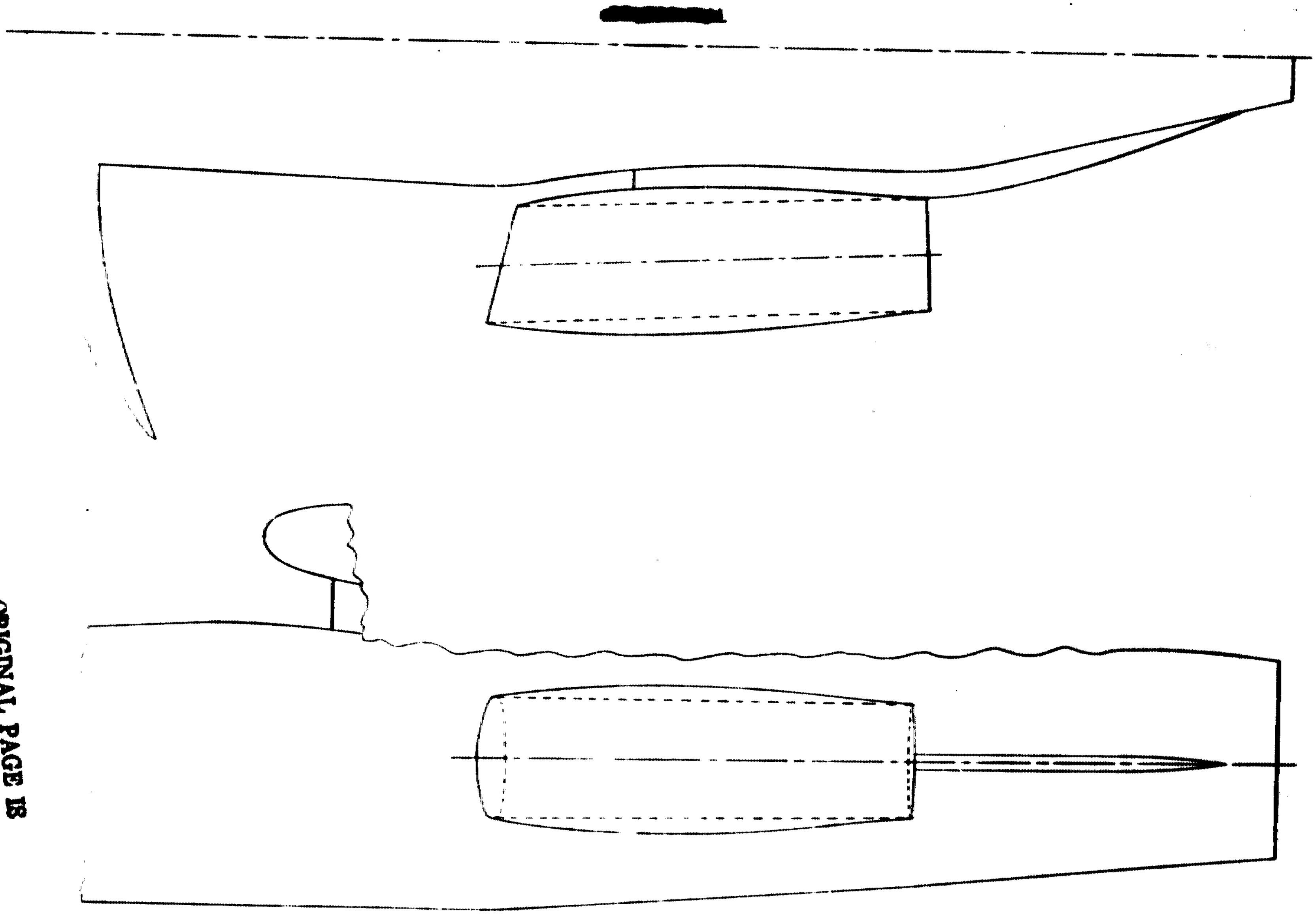

(a) Basic configuration.

Figure 1.- Model drawings.

[redacted]

[redacted]

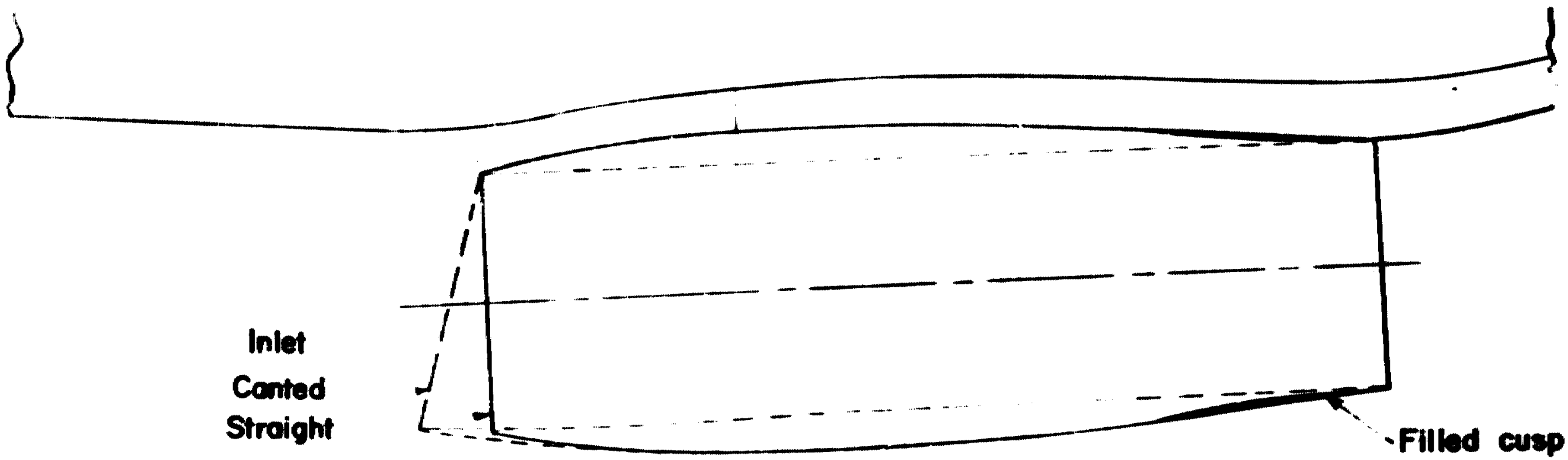

(b) Flow-through nacelle.

[redacted]

Figure 1.- Continued.

[redacted]

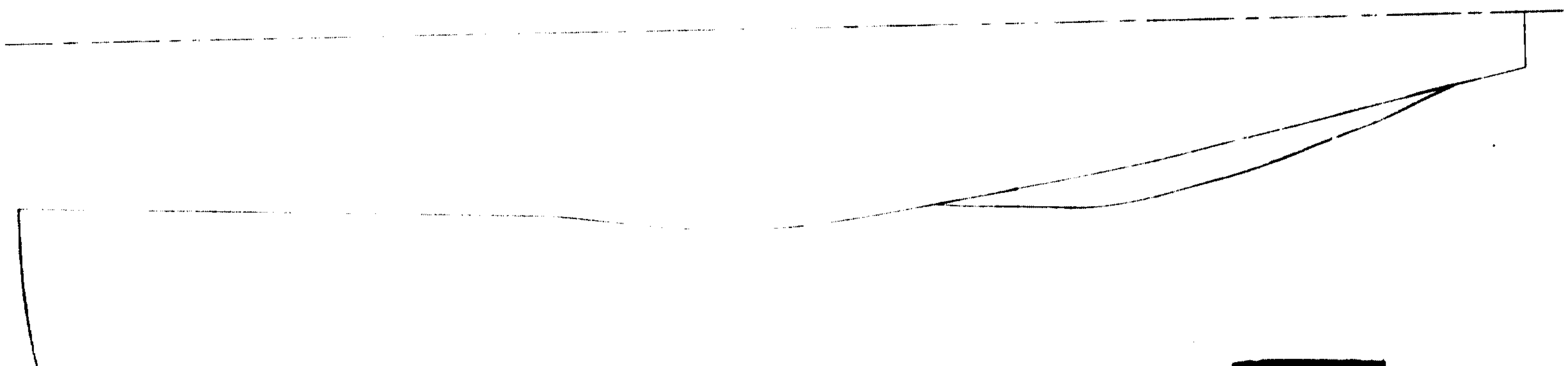

[redacted]

(c) Equivalent body configuration.

Figure 1.- Concluded.

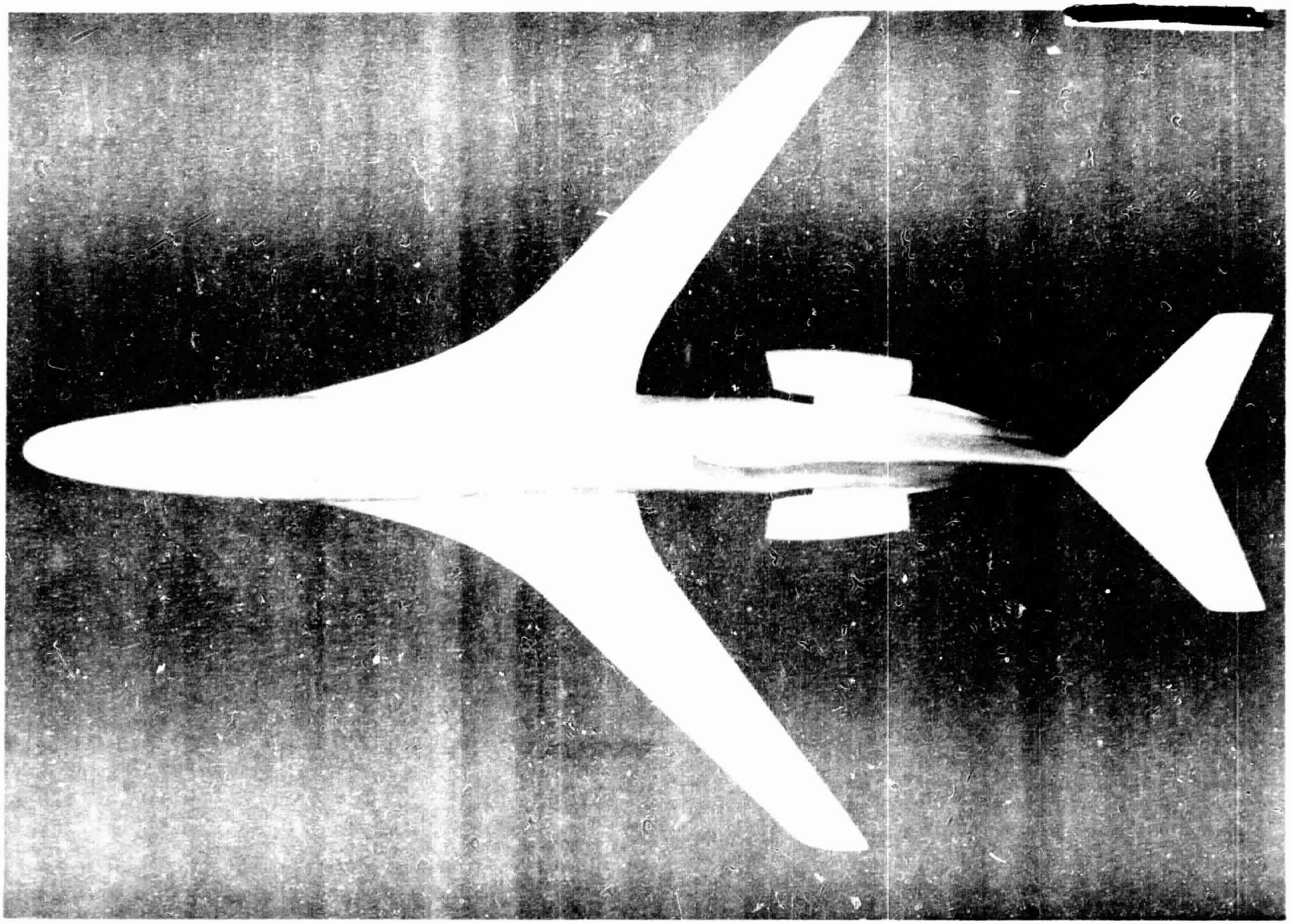

[redacted]

(a) Plan view.

Figure 2.- Model photographs.

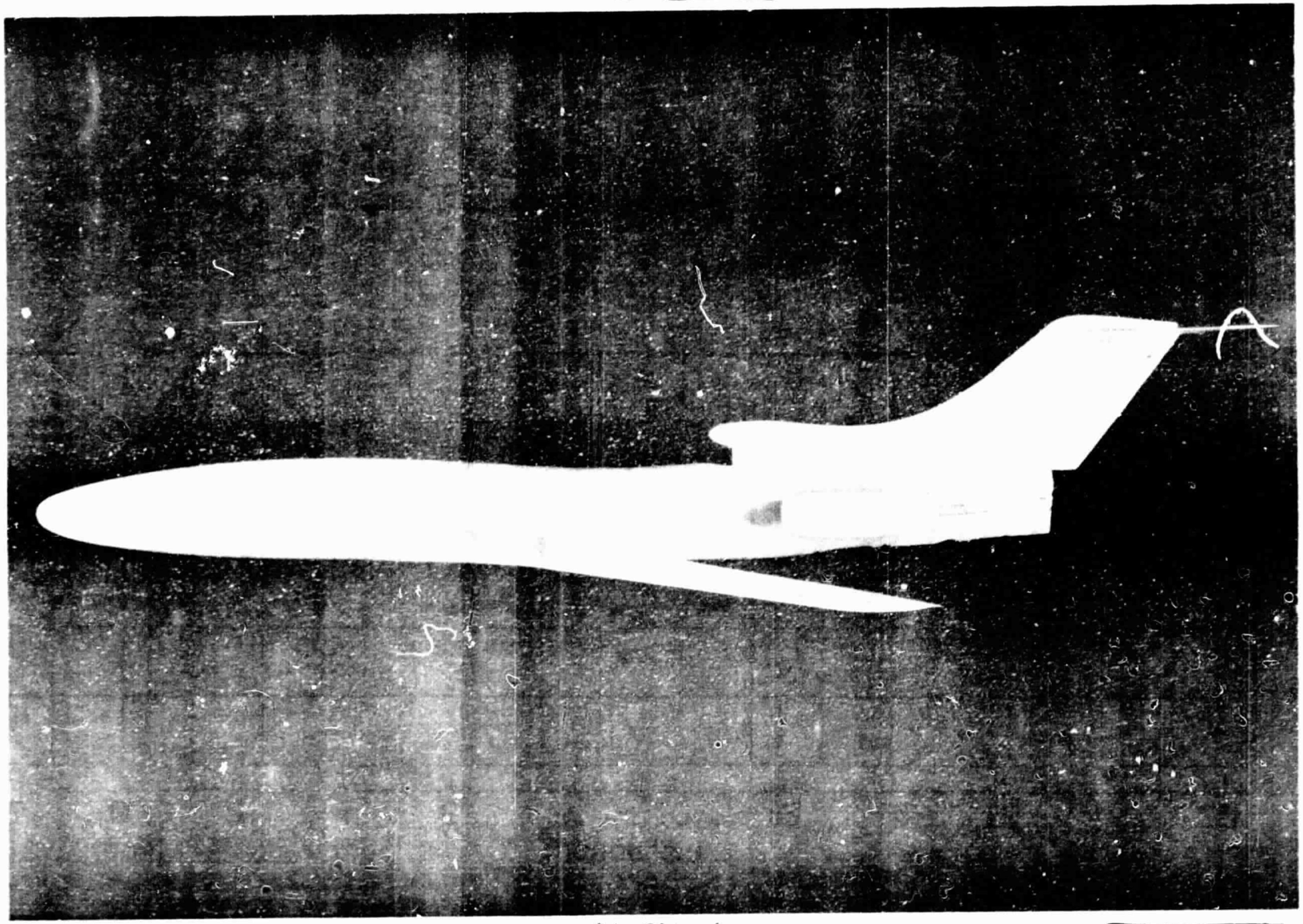

NASA
L-70-8672

(b) Side view.

Figure 2.- Concluded.

[redacted]

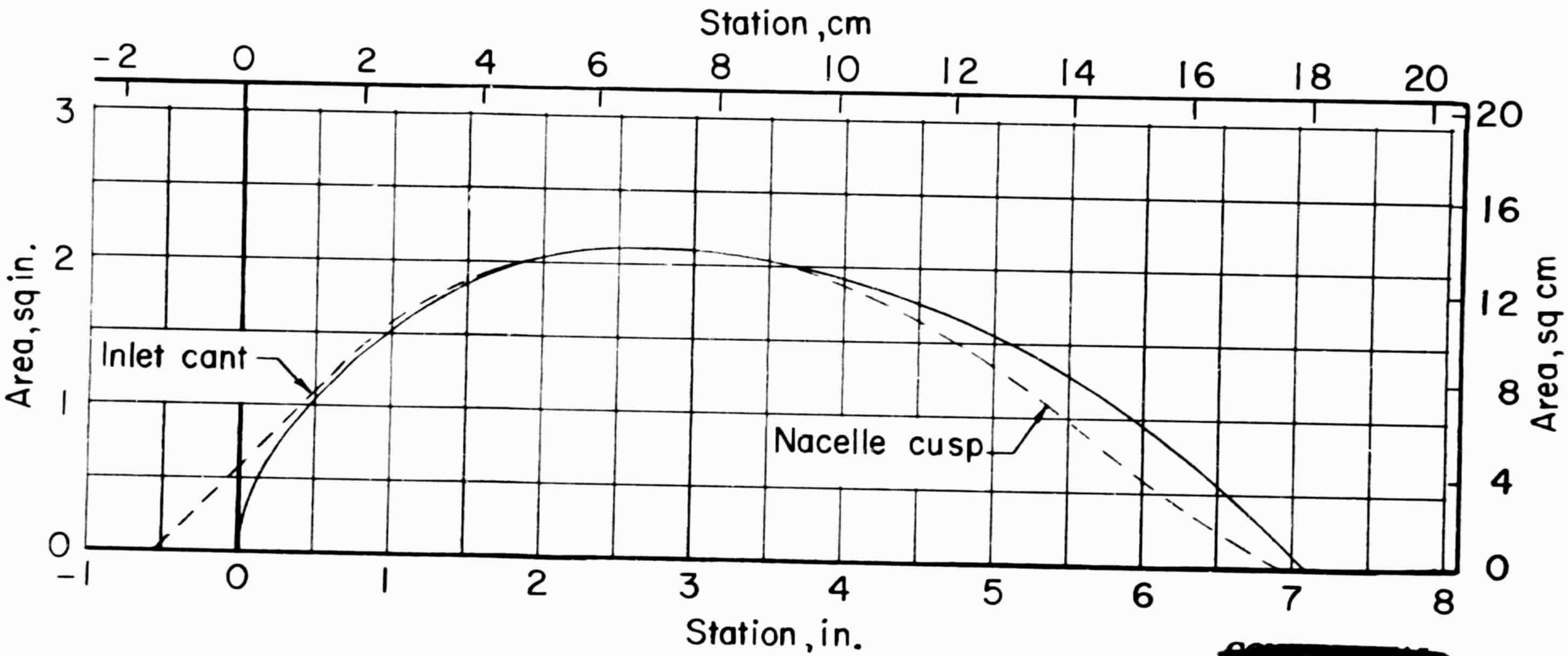

[redacted]

Figure 3.- Flow-through nacelle area distribution (stream tube area removed).

[redacted]

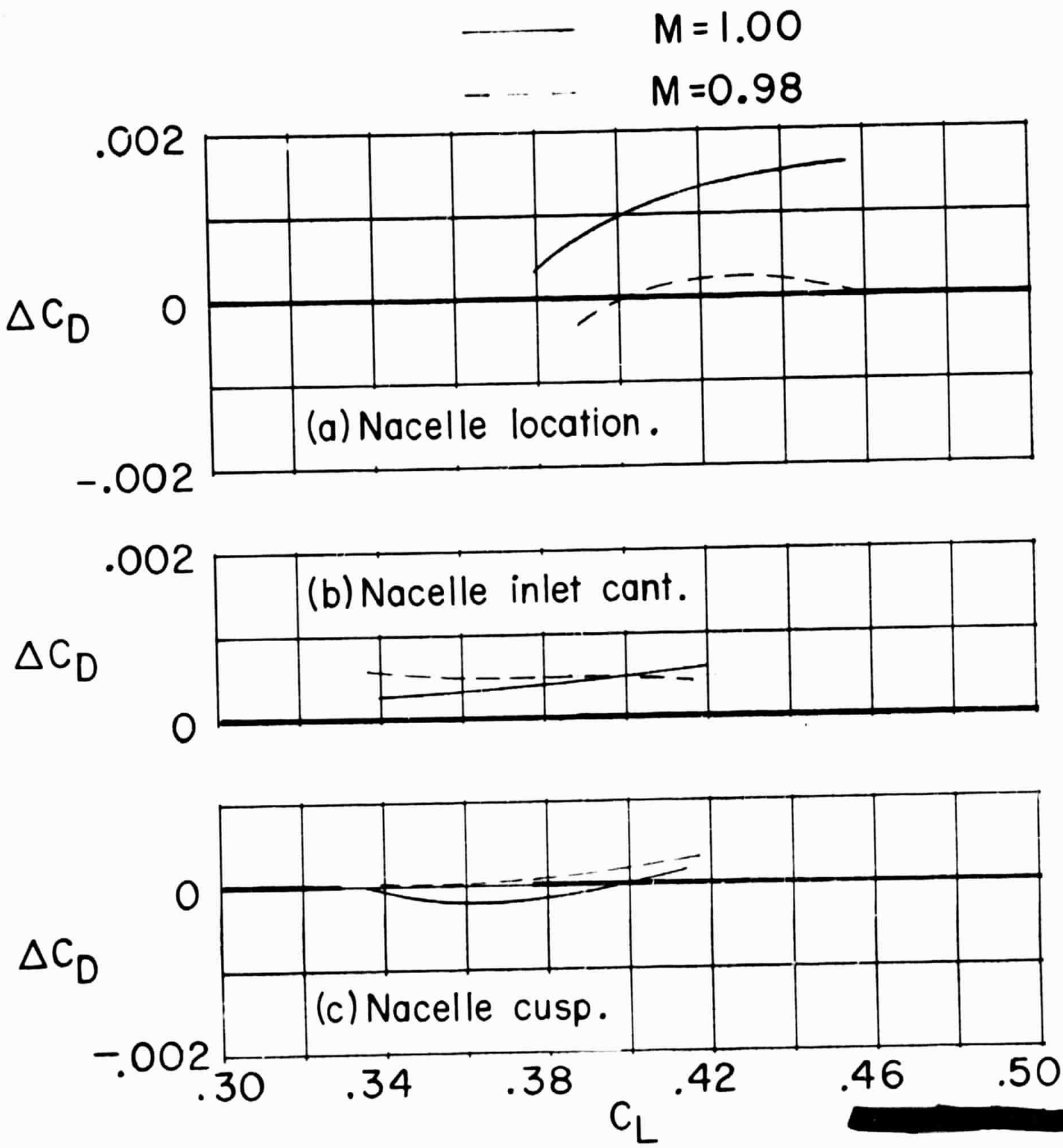

[redacted]

Figure 4.- Variation of drag differential with lift coefficient.

[redacted]

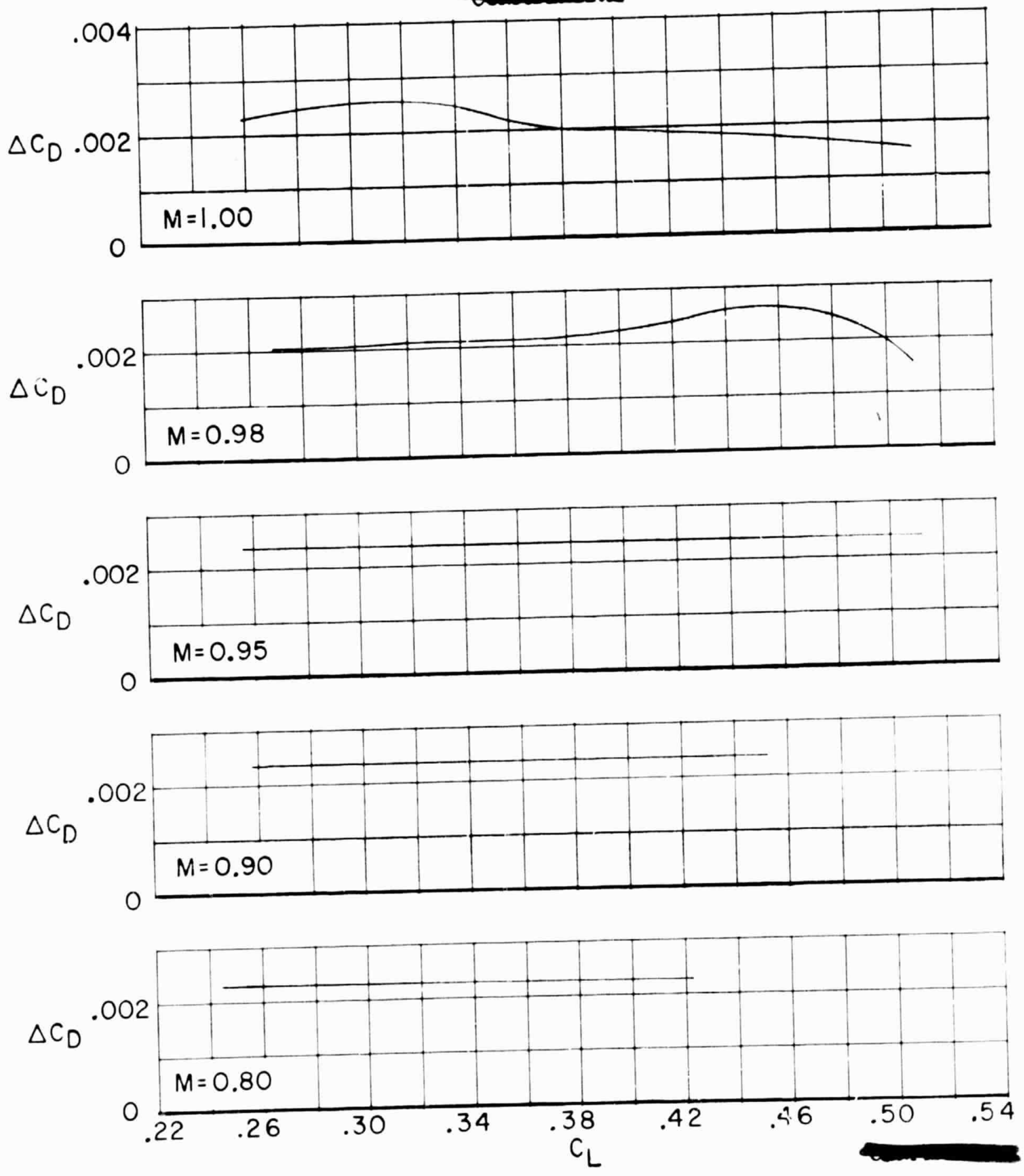

[redacted]

Figure 5.- Variation of drag differential with lift coefficient. Equivalent body.

[redacted]

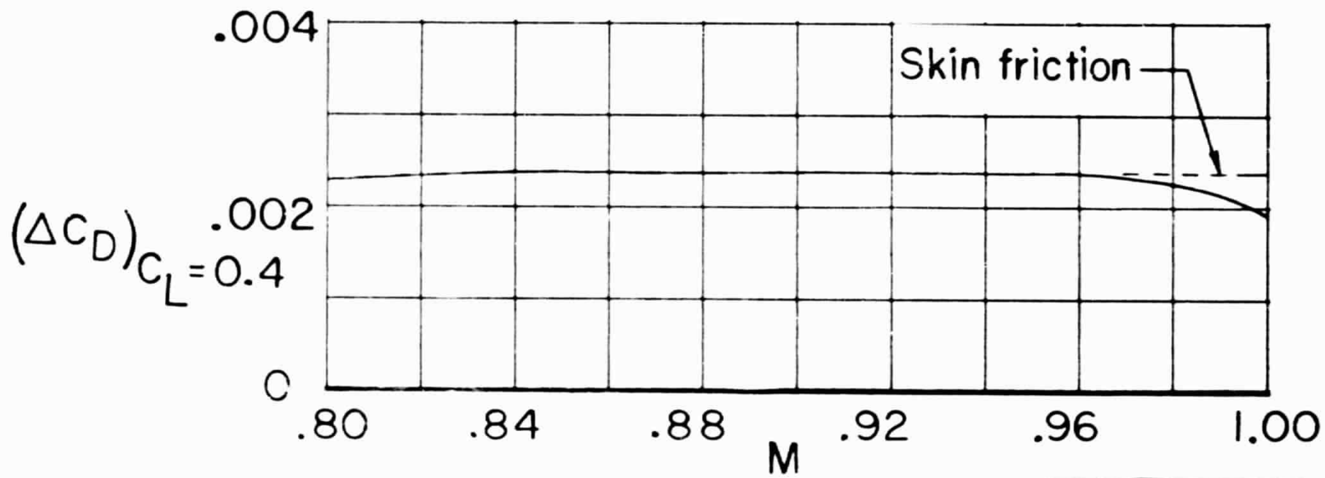

[redacted]

Figure 6.- Variation of drag differential with Mach number at 0.4 lift coefficient. Equivalent body.